Quantum Electronics **46** (11) 1047–1054 (2016)

SPECKLE SPECTROSCOPY DOI: 10.1070/QEL16193

Speckle spectroscopy of fluorescent randomly inhomogeneous media

D.A. Zimnyakov, I.A. Asharchuk, S.A. Yuvchenko, A.P. Sviridov

Abstract. **We propose a coherence optical method for probing fluorescent randomly inhomogeneous media based on the statistical analysis of spatial fluctuations of spectrally selected fluorescence radiation. We develop a phenomenological model that interrelates the flicker index of the spatial distribution of the fluorescence intensity at a fixed wavelength and the mean path difference of partial components of the fluorescence radiation field in the probed medium. The results of experimental approbation of the developed method using the layers of densely packed silicon dioxide particles saturated with the aqueous rhodamine 6G solution with a high concentration of the dye are presented. The experimentally observed significant decrease in the flicker index under the wavelength tuning from the edges of the fluorescence spectrum towards it central part is presumably a manifestation of spectrally dependent negative absorption in the medium.**

Keywords: *fluorescence, randomly inhomogeneous medium, narrow-band filtering, coherence, speckles.*

1. Introduction

To date, the coherence optical methods of probing randomly inhomogeneous media are the most efficient and demanded in the optical diagnostics of objects possessing a complex structure and dynamics. These methods include, e.g., different modifications of diffusing-wave spectroscopy, based on the correlation analysis of laser radiation scattered by the probed medium [1–10]. In this case, the diagnosed quantities are the parameters that characterise the dynamics of the scatterers in the medium having the spatial scale comparable with the wavelength of the probe radiation.

In application to the studies of the medium structure and the peculiarities of its interaction with the probe radiation, a different group of coherence optical methods is of interest. These methods are based on the analysis of the statistical characteristics of stochastic interference patterns formed by multiple scattering of laser or narrow-band thermal radiation by the probed objects. In particular, a method for probing randomly inhomogeneous media using the contrast measurement in multiply scattered speckle-modulated laser radiation was proposed in Ref. [11]. Based on the general principles of stochastic interference of partial components of the scattered light field in randomly inhomogeneous media, one can expect that the maximal sensitivity of the contrast used as a diagnostic parameter would be achieved in the case, when the coherence length of the probe radiation is comparable with its characteristic propagation path length $\tilde{s}$. In Ref. [12], the approach to the speckle-contrast diagnostics of randomly inhomogeneous media, using the probe radiation with tunable spectrum (and, therefore, the variable coherence length) is considered. The required effect in this case is achieved at the expense of varying the pump current of the semiconductor laser, operating in the subthreshold regime near the oscillation threshold. This technique allows the variation in the coherence length of the probe radiation within the interval from 25–30 μm to 3–4 mm (depending on the cavity length of the semiconductor laser). In this case, a characteristic feature is the mode structure of the radiation spectrum with the envelope shape close to Lorentzian. The variations in the pump current lead to the change in the envelope half-width that determines the coherence length of the probe radiation. The periodicity of the radiation mode structure in the subthreshold regime restricts the range of possible values of $\tilde{s}$ from above by nearly $\lambda^2/2\Delta\lambda_m$, where λ is the wavelength, and $\Delta\lambda_m$ is the intermode separation.

The speckle contrast probing can be also implemented using the frequency-modulated laser radiation under the condition that the modulation period is essentially smaller than the exposure time in the case of recording the speckle-modulated scattered radiation by means of a multielement photodetector. In the simplest case of binary frequency modulation, achieved as a result of periodical switching a single-mode semiconductor laser between the oscillation modes (e.g., using an oscillating diffraction grating as an external cavity mirror) the effective coherence function of the probing radiation can be presented by a harmonic function [13].

It is worth noting that certain analogies can be found between such methods and the low-coherence reflectometry of randomly inhomogeneous media [14] that uses the principles of optical coherence tomography [15]. In both cases, the informative signals are formed as a result of stochastic interference of a part of light waves, propagating in the medium along random paths and satisfying the necessary condition that the path difference of the waves should be smaller than the coherence length. At the same time, in contrast to the low-

D.A. Zimnyakov Yuri Gagarin State Technical University of Saratov, ul. Politekhnicheskaya 77, 410054 Saratov, Russia; Institute of Precision Mechanics and Control, Russian Academy of Sciences, ul. Rabochaya 24, 410024 Saratov, Russia; e-mail: zimnykov@mail.ru;
I.A. Asharchuk, A.P. Sviridov Federal Scientific Research Centre 'Crystallography and Photonics', Russian Academy of Sciences, Leninsky prosp. 59, 119333 Moscow, Russia;
S.A. Yuvchenko Yuri Gagarin State Technical University of Saratov, ul. Politekhnicheskaya 77, 410054 Saratov, Russia

Received 8 August 2016; revision received 7 October 2016
Kvantovaya Elektronika **46** (11) 1047–1054 (2016)
Translated by V.L. Derbov

coherence reflectometry using a reference beam with regular spatial structure, the discussed methods can be classified as 'reference-free low-coherence interferometry'.

The paper presents the results of experimental approbation and interpretation of the obtained experimental data for the specific case of speckle contrast probing, when the medium itself produces the probe radiation, fluorescing under pumping by cw laser radiation in the absorption band of the fluorophore. The coherence length of the recorded radiation, necessary for producing expressed speckle modulation of the fluorescence signal is achieved by narrow-band spectral filtering at the detection stage. Note that the proposed method is interesting not only from the point of view of further development of the speckle-contrast diagnostics of randomly inhomogeneous media. In relation to the intense development of fluorescence diagnostics methods for various applications in biomedicine and material science during three last decades (see, e.g., [16–20]), the use of spectral selection of fluorescence radiation in combination with the statistical analysis of intensity fluctuations, caused by the stochastic interference, can be also a subject of significant interest.

2. Phenomenological model of speckle spectroscopy in a randomly inhomogeneous medium

Let us accept the following model for further analysis.

(i) The fluorescent randomly inhomogeneous medium is pumped by cw laser radiation within the fluorophore absorption band, characterised by high efficiency of pump radiation absorption, due to which the absorption of laser radiation and the subsequent fluorescence occur within a sufficiently thin near-surface layer of the medium.

(ii) The fluorescence radiation is multiply scattered within the medium layer before it arrives at the detector, recording the fluorescence signal from the depths, exceeding the thickness of the pumped layer. The process of signal propagation can be described within the frameworks of the radiation transfer theory (RTT) [21].

(iii) In the course of detection, the spectral selection of the radiation by a rectangular window with the width $\Delta\lambda$ and the centre wavelength λ_c ($\Delta\lambda \ll \lambda_c$) is implemented.

Within the frameworks of this model, we do not consider the process of conversion of the pump radiation into the fluorescence one and focus our attention on the result of propagation of fluorescence radiation from the secondary sources in the near-surface medium layer to the detector under the condition of narrow-band spectral filtering.

In this formulation, the problem can be reduced to the case of probing a randomly inhomogeneous layer by narrow-band radiation having the coherence length $l_{coh} = \lambda_c^2/\Delta\lambda$. According to Ref. [12], the flicker index $\beta_I = \sigma_I^2/\langle I\rangle^2$ of multiply scattered linearly polarised radiation is described by the expression:

$$\beta_{I\mathrm{lp}} = \int_0^\infty \left| g(l_{coh}, \Delta s)\right|^2 \rho(\Delta s)\,\mathrm{d}(\Delta s). \tag{1}$$

Here, σ_I^2 and $\langle I\rangle^2$ are the spatial fluctuation variance and the mean intensity of the scattered quasi-monochromatic light, respectively; and $|g(l_{coh}, \Delta s)|$ is the modulus of the coherence function of the probe radiation that controls the modulation depth of the spatial intensity fluctuations in the course of stochastic interference of the scattered light field partial components. The complex-valued function $g(l_{coh}, \Delta s)$ is defined as the Fourier transform of the probe radiation spectral density at the output of the probed medium (with its narrow-band spectral filtering before the detection taken into account). In Eqn (1), $\rho(\Delta s)$ is the probability density function for the values of the path length difference of the partial components of the scattered length in the probed medium. The subscript *lp* corresponds to the case of detecting the linear multiply scattered light with the arbitrarily chosen polarisation azimuth. Note that the flicker index is uniquely related to the contrast value V of the stochastic interference patterns (speckle fields), also frequently used for their quantitative description, $\beta_I = V^2$.

In the case of detecting multiply scattered fluorescence radiation in the absence of polarisation discrimination (selection of linearly polarised component), one should keep in mind that the detected signal can be considered as a result of incoherent superposition of two linearly polarised statistically independent components (polarisation modes) with orthogonal directions of polarisation. Assuming the identical statistical properties of the random intensity values for these polarisation modes of the radiation, propagating in the randomly inhomogeneous medium, we obtain the flicker index of the resulting signal in the form

$$\beta_{I\Sigma} = \frac{(\sigma^2_{I\mathrm{lp}||} + \sigma^2_{I\mathrm{lp}\perp})}{(\langle I_{\mathrm{lp}||}\rangle + \langle I_{\mathrm{lp}\perp}\rangle)^2} = 0.5\frac{\sigma^2_{I\mathrm{lp}||}}{\langle I_{\mathrm{lp}||}\rangle^2} = 0.5\frac{\sigma^2_{I\mathrm{lp}\perp}}{\langle I_{\mathrm{lp}\perp}\rangle^2}, \tag{2}$$

where the symbols ||, $\perp$ relate to the corresponding polarisation modes. Thus, Eqn (1) should be modified in the following way:

$$\beta_{I\Sigma} = 0.5\int_0^\infty \left| g(l_{coh}, \Delta s)\right|^2 \rho(\Delta s)\,\mathrm{d}(\Delta s). \tag{3}$$

Below the subscript Σ will be omitted.

Consider the particular limiting cases of detecting the fluorescence light with a high and low degree of temporal coherence. The notions of 'high' and 'low' degree of spatial coherence should be considered from the point of view of the relation between l_{coh} and the mean value $\langle\Delta s\rangle$ of the path length difference of interfering partial components of the fluorescence radiation in the medium. For $l_{coh} \gg \langle\Delta s\rangle$ (high degree of coherence), $|g(l_{coh}, \Delta s)| \approx 1$ in the entire interval of possible values of $\langle\Delta s\rangle$, and, correspondingly, $\beta_I \approx 0.5$. Note that this situation corresponds to the case of overlapping of two orthogonally polarised statistically independent developed speckle fields and is described by the Rayleigh distribution of the local intensity values [22]:

$$\rho(I(\lambda)) = [2/\langle I(\lambda)\rangle]^2 I(\lambda)\exp[-2I(\lambda)/\langle I(\lambda)\rangle]. \tag{4}$$

On the contrary, when $l_{coh} \ll \langle\Delta s\rangle$, the observed spatial distribution of the local intensity values of the scattered radiation will be described by the Gaussian statistics with small values of the flicker index β_I. For $l_{coh}/\langle\Delta s\rangle \to 0$ the spatial distribution is close to uniform.

The probability density function for the values of the path length difference of the field partial components for the fluorescence radiation in the medium $\rho(\Delta s)$ can be written as [12, 13]

$$\rho(\Delta s) = K\int_0^\infty \rho(s + \Delta s)\rho(s)\,\mathrm{d}s, \tag{5}$$

where K is the normalisation coefficient, determined from the condition

$$K\int_0^\infty \rho(\Delta s)\,\mathrm{d}(\Delta s) = 1.$$

Under the fixed conditions of excitation and detection of fluorescence, the probability density function $\rho(s)$ is determined by the shape of the light pulse $\delta(t)$, recorded by the detector under the excitation of fluorescence by an ultrashort pump pulse $I(t) \backsim \delta(t)$ (provided that the spread of emission times after the excitation is essentially smaller that the characteristic time of light propagation from the emitter to the detector). Depending on the optical characteristics and geometry of the medium, the function $\rho(s)$ can be obtained either by approximate analytical solution of the time-dependent equation of radiation diffusion, or by numerical solution of the radiation transfer equation (RTE) [21]. One of the approaches to solving the RTE numerically is the simulation of radiation transfer in the medium using the Mote Carlo method, which is used to obtain $\rho(s)$ in the present paper.

From the rectangular shape of the spectral window used in the considered case for narrow-band filtering of the fluorescence radiation it follows that the modulus of the coherence function can be presented as

$$|\,g(l_{\mathrm{coh}}, \Delta s)\,| = \left|\,\mathrm{sinc}\left(\pi\frac{\Delta s}{l_{\mathrm{coh}}}\right)\right|. \qquad (6)$$

3. Experimental technique and results

In our case the samples under study were layers of densely packed nanoporous particles of SiO_2 having irregular shape (Fig. 1). The statistical analysis of electron microscopy images of individual particles, performed for the sample of 200 fragments of individual images, allowed the estimation of the mean values and the root-mean-square deviation for the geometrical cross section of the particles, approximately equal to 1.95×10^4 μm^2 and 7.23×10^3 μm^2, respectively. The used silicon dioxide powder was kept in cylindrical metallic containers having the height 2 mm and the inner diameter 5 mm, placed on glass substrates, and was slightly compressed to obtain flat surfaces. The volumetric analysis of the samples has shown that the volume fraction of SiO_2 particles in the layers is nearly 0.35. The layers were saturated with the aqueous solutions of rhodamine 6G with the volume fraction of the dye in the layer equal to 0.005.

The dye fluorescence in the surface zone of the layers (Fig. 2) was excited by cw laser radiation having the wavelength 532 nm (diode-pumped solid-state Nd:YAG laser). The beam of laser radiation was extended using the defocusing lens with the focal length 200 mm and was incident onto the surface of the layer at an angle of 45°, completely overlapping it. The power density of pump radiation at the surface of the layer was estimated as 80 mW cm^{-2}. To record the fluorescence radiation in the layer we used the confocal Raman microscope (LabRam GR800, Horiba Jobin Yvon). In the course of the experiment, the layers were scanned in the directions parallel to the surface at the depths h = 50, 100, 150 and 200 μm. The length of the individual scan trace was 1 mm and the scanning step was 10 μm. For each depth, the number of non-coincident scanning traces was equal to 20. At each step, the fluorescence spectra were recorded within the wavelength interval 570–700 nm with the slit width 0.052 nm. To eliminate the pump radiation, we used the optical filter blocking the radiation with the wavelengths shorter than 533 nm in the optical scheme of the microscope sed. The small slit width of the Raman microscope monochromator used for spectral selection of the fluorescence radiation allowed one to obtain sufficiently large coherence lengths of the detected radiation (6.25 mm for the high-frequency edge of the emission spectrum at 570 nm and 9.42 mm at 700 nm). The transverse size of the detection zone in the sample volume for the used confo-

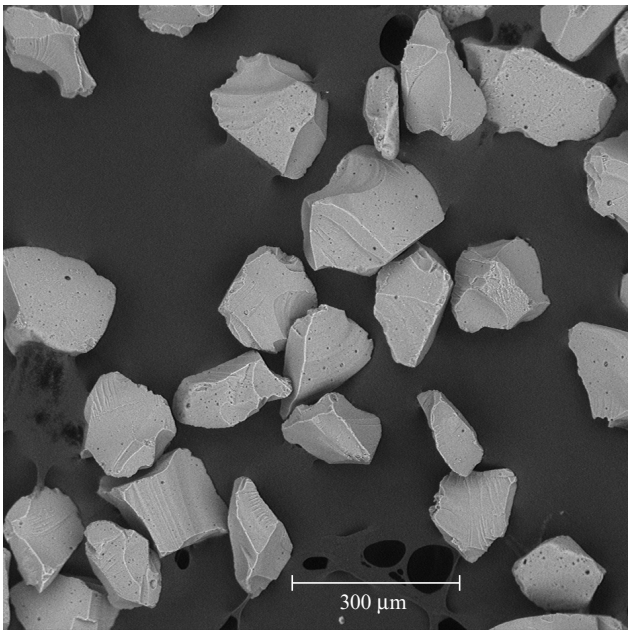

Figure 1. Electron microscopy image of SiO_2 particles used to prepare the samples.

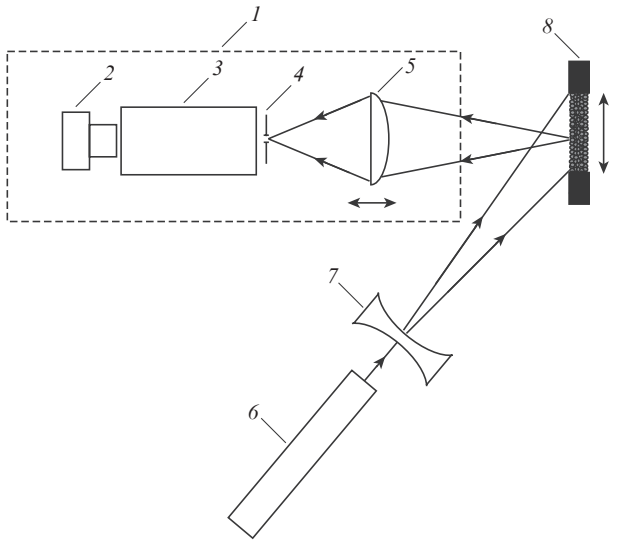

Figure 2. Schematic of the experimental setup:
(*1*) optical system of the confocal Raman microscope; (*2*) CCD photodetector; (*3*) monochromator; (*4*) pinhole aperture; (*5*) microscope objective; (*6*) diode pumped solid-state laser; (*7*) defocusing lens; (*8*) studied sample in the container.

cal systems, consisting of a pinhole aperture and a microscope objective, did not exceed 2 μm.

In the course of experiments, the following features of spatio-spectral distributions of the recorded fluorescence signals were revealed.

The fluorescence spectra of the studied samples, recorded at different points of the scanning traces are characterised by sufficiently high variability of the wavelength position and value of maxima. The averaged value of the wavelengths corresponding to the fluorescence maxima $\langle\lambda_{max}\rangle \approx 596.5$ nm, and the mean square deviation of maxima from $\langle\lambda_{max}\rangle$ is approximately 14.8 nm. All local spectra of fluorescence, recorded within the layer volume, are essentially shifted towards the long-wavelength region as compared to the reference spectrum. For the latter we took the fluorescence spectrum of the used aqueous dye solution. The mean shift value is approximately 37.8 nm.

The spatial distributions of the fluorescence intensity at fixed wavelength demonstrate high stochasticity (Fig. 3) with the modulation depth essentially dependent on the wavelength. The depth of the stochastic modulation decreases from the edges of the fluorescence spectrum to its central part.

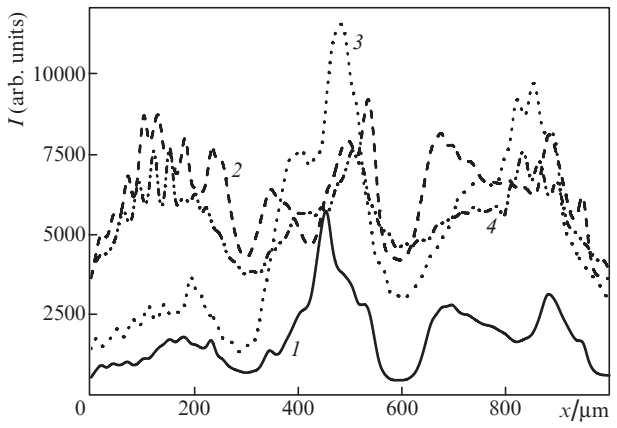

Figure 3. Fluorescence intensity distributions at fixed wavelengths along the scanning traces for the scanning depth $h = (1, 2)$ 50 and $(3, 4)$ 150 μm at $\lambda_c = (1)$ 565.40, (2) 632.10, (3) 570.49 and (4) 637.51 nm.

The statistical characteristics of the variability of the local fluorescence spectra, as well as those of the spatial fluctuations of the fluorescence intensity at a fixed wavelength (the mean values and the variances) insignificantly change with the change in the scanning depth within the used interval 50–200 μm. In this relation, in the statistical analysis of the spatial intensity fluctuations for different fixed wavelengths, the averaging was performed not only over different scanning traces for λ_c from the specified depth, but also over the different probing depths.

Figure 4 presents the spectral dependences of the flicker index $\beta_I(\lambda_c)$, demonstrating the above weak dependence on the probing depth h. The inessential spread of β_I for different h has no systematic character and seems to be determined by the sampling volume limitation. The confidence intervals for the dependence $\beta_I(\lambda_c)$ for uniformly distributed wavelengths in the interval 570–700 nm, corresponding to the confidence level 0.9 (Fig. 5), illustrate the spread in the values of $\langle\beta_I\rangle$ calculated from the experimental data and averaged over the probed volume. Figure 5 also presents the fluorescence spectrum $\langle I(\lambda_c)\rangle/\langle I_{max}(\lambda_c)\rangle$ normalised to the maximal value. A characteristic feature is that the minimal value of the flicker index is achieved closer to the inflection point of the fluorescence spectrum $\langle I(\lambda)\rangle/\langle I_{max}(\lambda)\rangle$, rather than near its maximum.

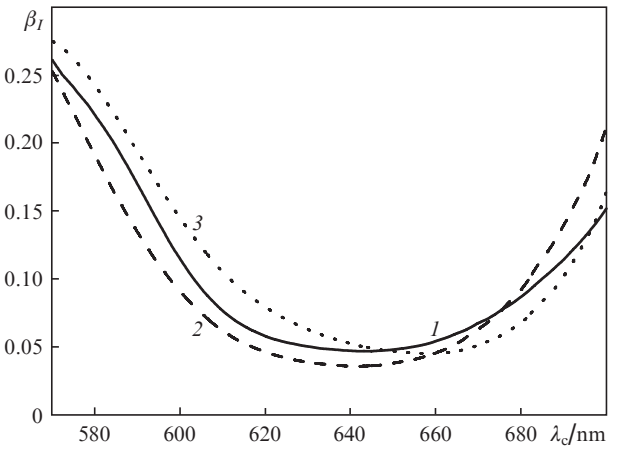

Figure 4. Spectral dependences of the flicker index for the spatial intensity distributions at the porbing depths $h = (1)$ 50, (2) 150 and (3) 200 μm.

One should also note the existence of periodic low-amplitude oscillations, manifesting themselves in the spectral region of the maximal values of the fluorescence intensity for different positions of the detection zone. These oscillations have the interference nature, do not relate to the studied samples, and are probably due to the parasitic interference in the optical scheme of the confocal Raman microscope.

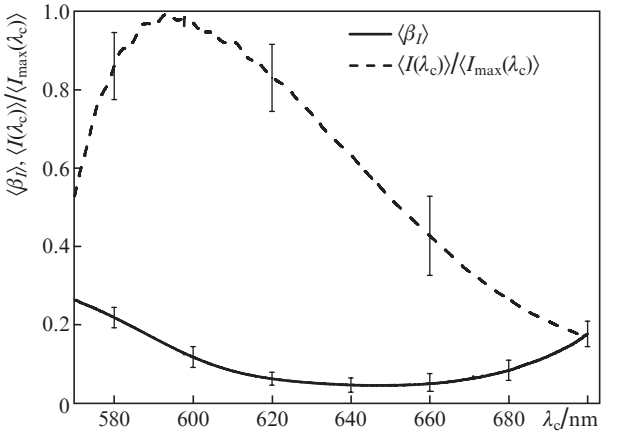

Figure 5. Dependence $\beta_I(\lambda_c)$ and fluorescence spectrum normalised to the maximal value, averaged over different probing depths. The confidence intervals are shown for the selected wavelengths and correspond to the confidence level 0.9.

4. Discussion of experimental results

The effect of an essential decrease in the flicker index β_I under wavelength tuning towards the centre of the spectrum $\langle I(\lambda)\rangle/\langle I(\lambda_{max})\rangle$, observed in the experiment (see Fig. 5), within the considered approach is due to an essential increase in the quantity

$$\langle \Delta s \rangle = \int_0^\infty \Delta s \, \rho(\Delta s) \mathrm{d}(\Delta s).$$

Due to its coarse-grained structure, the probed medium should be characterised by sufficiently large transport length l^* of the radiation propagation in the medium and the scattering anisotropy parameter g [21]. In particular, the preliminary estimates of these parameters for the disordered system of SiO_2 spherical scatterers in water with the same geometric cross section as that of the particles of the studied system, averaged over the ensemble, and the same volume fraction of particles, yield the value of l^* in the interval 10–30 mm and $g \sim 0.95–0.97$. However, we should note that the extremely irregular shape of particles in our case, characterised by the presence of multiple ribs and angles, as well as the nanoporosity of the particles, could lead to the essential decrease in the transport length values for the studied system as compared to the above estimate data. Nevertheless, for the considered spectral interval the value of l^* should be large enough, and, as shown below, comparable with the layer thickness.

For a 'passive' randomly inhomogeneous medium in the absence of fluorescence radiation, the essential increase in $\langle \Delta s \rangle$ for the probe radiation in a certain wavelength interval is expected to be caused by strong dependence of its optical transport parameters (the transport length, the scattering anisotropy parameter, and the absorption length) on the wavelength in this interval. However, no such behaviour is observed. Note also that the absorption of light by the considered system in the interval 600–700 nm is rather small. The increase in the coherence length of the detected radiation with increasing wavelength at the constant width of the spectral window should lead to the effect, opposite to the one observed at the value of $\langle \Delta s \rangle$ unchanged (the values of β_I for the long-wavelength edge of the fluorescence spectrum should be larger than for the short-wavelength one). The broadening of the distribution $\rho(s)$ of partial components over the propagation lengths in the medium and, hence, the growth of $\langle \Delta s \rangle$ can be efficiently caused by the negative absorption (gain) of the radiation propagating through the medium. In this case, the function $\rho(s)$ is subjected to the following transformation: $\rho(s) \to \rho(s)\exp(\tilde{\mu}_a s)$, where $\tilde{\mu}_a$ is the negative absorption coefficient. Such a transformation leads to an increase in the contributions to the fluorescence signal from the partial components with large values of s. The appearance of the negative absorption in the wavelength interval, corresponding to the central part of the fluorescence spectrum $\langle I(\lambda) \rangle / \langle I(\lambda_{max}) \rangle$, could be caused by the high concentration of the dye in the system, increasing the probability of manifestation of elementary processes of stimulated emission in the propagation of the partial components through the medium.

For quantitative estimation of the effect of the parameter $\langle \Delta s \rangle$ and the hypothetic spectrally dependent negative absorption on the flicker index of the detected fluorescence signal, we applied the Monte Carlo simulation of the radiation transfer in the randomly inhomogeneous layer. The simulation procedure, analogous to the one described previously [12, 13], was modified to allow for the specific features of the fluorescence emission and detection. Due to the extremely high concentration of the dye in the solution, the estimated thickness of the layer, in which the pump radiation is converted into the fluorescence radiation, amounts to a few micrometres only [23], whereas the registration of the fluorescence signal is carried out in much deeper layers. In the Monte Carlo simulation we used the approach, in which the medium absorption (positive or negative) is taken into account by multiplying the weight of the propagating 'photon' packet by the Bouguer factor $\exp(-\mu_a s)$. Within the framework of this approach, the weight of the packet propagating through the medium between the emitting region and the detector by the distance s is determined by the probability density $\rho(s)$. At the initial stage, the simulation is performed with the unabsorbing randomly inhomogeneous medium, after which the obtained probability density function $\rho(s)$ is transformed using the Bouguer factor to take the absorption into account.

In the course of simulation, the phase function of the medium [21] was taken in the Henyey–Greenstein form [24], adequately describing the angular distributions of the scattered radiation intensity for the randomly inhomogeneous media of different types practically in the entire range of possible values of the scattering anisotropy parameter g (except a small region in the vicinity of unity). At the first stage of simulation we studied the interrelation between the values of l^* and $\langle \Delta s \rangle$ for planar unabsorbing randomly inhomogeneous layers with the thickness 2 mm with the scattering anisotropy parameter lying within the interval 0.80–0.97. The modelled scheme (the pumping of the near-surface region of the medium and the detection of radiation from a deeper located layer in the backscattering geometry) corresponded to the geometry of the experiment. The number N of 'photon' packets, injected into the medium, was equal to 10^6. The analysis of the output data demonstrated the absence of the procedure cycling with this N. Because of the absence of *a priori* values of the optical parameters of the studied system, in the course of simulation the value of l^* as an initial parameter of the procedure was chosen within the interval 0.05–25 mm (in order to overlap the unknown value of the transport length for the probed samples). As an example, Fig. 6 presents typical functions $\rho(s)$ and $\rho(\Delta s)$, obtained as a result of simulation of sets of random values of s for the 'photon' packets propagating through the medium. The functions $\rho(\Delta s)$ were calculated in correspondence with the expression (5), after which for the given values of l^* and g the quantity $\langle \Delta s \rangle$ was calculated.

The analysis of the obtained results revealed the weak dependence of $\langle \Delta s \rangle$ on the scattering anisotropy parameter, namely, when g varies within the interval 0.80–0.97 and $l^* =$ 25 mm, the corresponding values of $\langle \Delta s \rangle$ differ by no more

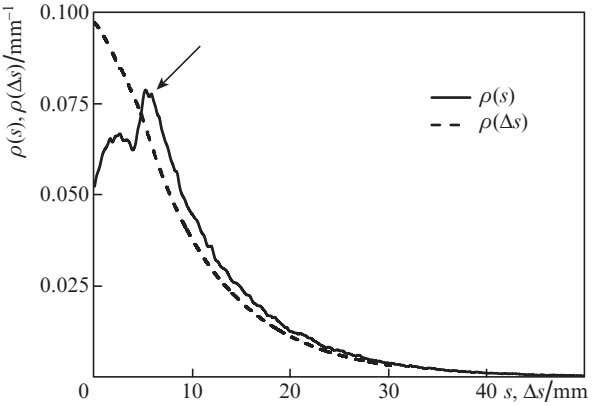

Figure 6. Examples of functions $\rho(s)$ and $\rho(\Delta s)$, obtained by the Mote Carlo simulation. The transport length is $l^* = 1.96$ mm. The arrow points to the peak, corresponding to the partial components of the fluorescence radiation field that undergo single scattering from the back surface of the layer.

than 5%–6% and become negligibly small at smaller values of l^*. This fact is probably caused by the diffusing regime of light propagation between the emitting region and the detector for the used detection scheme. In spite of the considerable contribution to the recorded signal from the partial components that have experienced single scattering from the lower boundary and propagate in the layer through relatively small distances (the corresponding peak in Fig. 6 is marked by an arrow), the model values of s for this peak essentially exceeds the doubled thickness of the layer. This indirectly confirms the diffusion character of the fluorescence radiation propagation in the layer.

Due to the weak dependence of $\langle \Delta s \rangle$ on g, at the second stage of the simulation the value of g was fixed to be 0.90, based on the following considerations. The above estimates for systems of coarse spherical SiO_2 particles yield the values of g close to 1. The expressed shape irregularity of the particles in the medium under study should lead to somewhat reduced scattering anisotropy, in spite of the extremely large value of the wave parameter of the scatterers $\pi a/\lambda \approx 600-800$ (here a is the characteristic particles size). The question arises whether the used approach, based on the radiation transfer theory, is applicable to such coarse-grained systems. It is worth noting that within the performed phenomenological analysis the evaluated parameters of radiation transfer in the medium (first of all, $\langle \Delta s \rangle$) are by no means related to the characteristics of individual scatterers (e.g., the scattering efficiency factor). Instead, they are interpreted basing on the integrated effects of interaction of the medium with radiation (stochastic interference with narrow-band filtering of multiply scattered fluorescence radiation). At the same time, the applicability of RTT to the description of radiation transfer in randomly inhomogeneous media using the optical transport parameters (transport length, scattering length and scattering anisotropy parameter) is still not disproved by anybody.

In further simulation, for different distributions $\rho(\Delta s)$ (and, correspondingly, different $\langle \Delta s \rangle$) using Eqns (3) and (6) we calculated the values of β_I as functions of the wavelength λ_c. The results are presented in Fig. 7 by the family of curves $\beta_I = f(\Delta s, \lambda_c)$, the difference of which is caused by the difference of the coherence lengths $l_{coh} = \lambda_c^2/\Delta\lambda$. The increase in the mean path difference for the partial components of the fluorescence field in the probed medium leads to fall of β_I; larger wavelengths correspond to larger β_I, which is due the larger coherence length of the detected radiation, the width of the spectral window being unchanged.

In the plots of Fig. 7 the points present the averaged values of β_I obtained in the experiment at the appropriate wavelengths. Note that in the case of a weak dependence of $\langle \Delta s \rangle$ on λ_c (or the absence of such dependence) for the system under study the experimental values would be localised in a compact area in the plane $(\langle \Delta s \rangle, \beta_I)$, and the variations of the flicker index under the monochromator wavelength tuning from 580 to 700 nm would not exceed 0.04–0.05. However, based on the obtained model dependences, the variations of β_I observed in the experiment with λ_c varying from 570 to 630 nm correspond to more than a quadruple increase in Δs. Such sharp broadening of the distribution $\rho(s)$ of partial components of the fluorescence radiation field over the path lengths in the medium within a sufficiently narrow spectral range cannot be explained within the concept of a 'passive' linear randomly inhomogeneous weakly absorbing medium, for which at the fixed thickness the main influence on Δs is exerted by the transport length l^*. The factor so cardinally affecting the statistics of partial component paths in the medium can be the spectrally dependent negative absorption, caused by the high concentration of the dye. Suppose that the coefficient of negative absorption $\tilde{\mu}_a$ that determines the amplification of the fluorescence radiation propagating through the medium tends to zero near the short-wavelength edge of the fluorescence spectrum and increases as the wavelength is shifted towards the central part of the spectrum. Within the considered model, the value $\Delta s \approx 8.5$ mm obtained for $\lambda_c = 700$ nm corresponds to the transport length $l^* \approx 1.96$ mm, comparable with the thickness of the studied samples.

Using the Mote Carlo method we simulated the effect of $\tilde{\mu}_a$ on Δs for the medium layer with the given value of l^*, assumed to correspond to the system studied here. Figure 8 illustrates the interrelation of $\tilde{\mu}_a$ and Δs; the inset shows the spectral dependence $\tilde{\mu}_a(\lambda)$ with the maximum near the inflection point of the normalised averaged fluorescence spectrum $\langle I(\lambda) \rangle / \langle I(\lambda_{max}) \rangle$. The analysis of interrelation between the values of $\tilde{\mu}_a(\lambda)$ and the first derivative $d/d\lambda \{\langle I(\lambda) \rangle / \langle I(\lambda_{max}) \rangle\}$ revealed rather large (about –0.8) Pearson correlation coeffi-

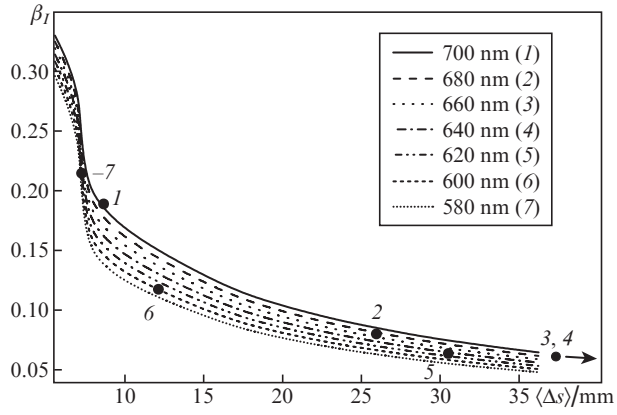

Figure 7. Theoretical dependences of β_I on $\langle \Delta s \rangle$ for different selected wavelengths λ_c. The point show the experimental values of the flicker index averaged over the probed volume [see the dependence $\beta_I(\lambda_c)$ in Fig. 4]. For λ_c equal to 630 and 640 nm the corresponding points are beyond the displayed interval of $\langle \Delta s \rangle$.

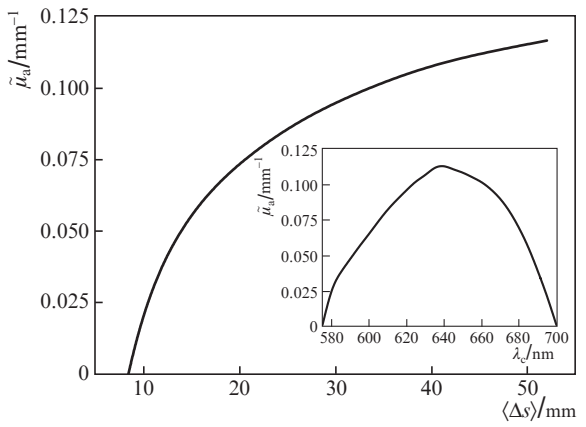

Figure 8. Calculated dependence of $\tilde{\mu}_a$ on $\langle \Delta s \rangle$ at $l^* = 1.96$ mm. The inset shows the spectrum of $\tilde{\mu}_a$, calculated within the frameworks of the proposed model based on the obtained experimental data.

cient (the negative sign corresponds to the growth of one quantity accompanied by a decrease in the other).

The conclusion about the existence of considerable spectrally dependent amplification of the fluorescence radiation in the coarse-grain medium pumped by cw laser radiation seems somewhat unexpected. As a rule, the effects of gain and generation of laser radiation in randomly inhomogeneous media are studied under pumping by pulsed laser light with much greater power densities of the order of a few MW mm^{-2} (see, e.g., [25]). However, it should be noted that the issues of the effect of spectrally dependent fluorescence yield on the diffusion transfer of the fluorescence radiation in a randomly inhomogeneous medium, similar to considered here essentially below the laser oscillation threshold, have not been especially considered until now. The system studied in the present paper is comparable with some studied random laser media in morphology and optical properties of the matrix medium (densely packed layers of silicon dioxide particles), the dye concentration being essentially higher [25]. In our opinion, an additional indirect argument in support of the hypothesis of the manifestation of the medium active properties in the diffusion transfer of the fluorescence radiation in the studied system is the strong correlation between the reconstructed values of $\widetilde{\mu}_a$ and the dispersion of the normalised fluorescence spectrum $\mathrm{d}/\mathrm{d}\lambda\,\{\langle I(\lambda)\rangle/\langle I(\lambda_{max})\rangle\}$.

Note that the essential effect on the transfer of the fluorescence radiation with the wavelengths shorter than 580 nm is also expected from the absorption of rhodamine 6G, corresponding to the low-frequency wing of the dye absorption spectrum. In our opinion, this is just the fact that explains the specific features of the β_I spectral dependences, observed in the experiment, namely, their asymmetry and the shift of the minimum towards the long-wavelength region with respect to the fluorescence maximum.

5. Conclusions

Thus, we have proposed a method for probing fluorescent randomly inhomogeneous media, based on the analysis of the spectral dependence of the flicker index of the recorded fluorescence signal subjected to narrow-band filtering. The developed phenomenological model allows the establishment of interrelation between the value of the flicker index at the fixed wavelength and the mean path difference of the partial components of the fluorescence radiation field in the medium. In turn, within the frameworks of the radiation transfer theory from the obtained mean path difference one can reconstruct the optical transport parameters of the probed medium. The application of the developed method to the fluorescent medium, pumped by a cw laser and consisting of densely packed grains of silicon dioxide, saturated with the aqueous solution of rhodamine 6G allowed the establishment of a strong dependence of the mean path difference of the partial components on the wavelength. The maximal value of the mean path difference is achieved near the inflection point of the fluorescence spectrum. Such features are likely due to the effect of spectrally dependent negative absorption (gain) of the fluorescence radiation in the studied system.

The results can serve as a physical base for the creation and development of new approaches in the fluorescence diagnostics for applications in biomedicine and material science. Like other optical diffusive methods (diffuse reflection and transmission spectroscopy, coherence backscattering spectroscopy [26, 27], low-coherence reflectometry [14]) and in combination with them, the speckle spectroscopy of scattered fluorescence radiation can be used to estimate the optical transport parameters of the probed medium. In turn, from the obtained values of transport parameters (transport length, scattering anisotropy parameter, effective refractive index) using the effective medium models (see, e.g., [27, 28]) one can evaluate the structure characteristics of the probed systems (the mean size of scattering centres, their concentration in the medium and refractive index at the wavelength of the probing radiation). The method of speckle spectroscopy of the scattered fluorescence radiation is applicable to different classes of scattering media (biological tissues, composite materials, polymer systems), provided that the characteristic propagation length of the fluorescence radiation in the medium is comparable with the coherence length of the detected radiation, determined by the width of the spectral window.

Acknowledgements. The work was supported by the Russian Science Foundation (Grant Nos 16-19-1045 and 14-25-00055) in the part concerning the construction of the experimental setup, fabrication of samples and conducting the experimental studies, and by the Ministry of Education and Science of Russia within the frameworks of the State Task on Conducting Scientific Research by the institutions of higher education (Grant No. 549) in the part concerning the theoretical analysis of the obtained data.

References

1. Pine D.J., Weitz D.A., Chaikin P.M., Herbolzheimer E. *Phys. Rev. Lett.*, **60**, 1134 (1988).
2. Lemieux P.-A., Vera M.U., Durian D.J. *Phys. Rev. E*, **57**, 4498 (1998).
3. Boas D.A., Campbell L.E., Yodh A.G. *Phys. Rev. Lett.*, **75**, 1855 (1995).
4. Boas D.A., Yodh A.G. *J. Opt. Soc. Am. A*, **14**, 192 (1997).
5. Bandyopadhyay R., Gittings A.S., Suh S.S., Dixon P.K., Durian D.J. *Rev. Sci. Instrum.*, **76**, 093110 (2005).
6. Viasnoff V., Lequeux F., Pine D.J. *Rev. Sci. Instrum.*, **73**, 2336 (2002).
7. Scheffold F., Romer S., Cardinaux F., Bissig H., Stradner A., Rojas-Ochoa L.F., Trappe V., Urban C., Skipetrov S.E., Cipelletti L., Schurtenberger P. *Prog. Colloid Polym. Sci.*, **123**, 141 (2004).
8. Brunel L., Brun A., Snabre P., Cipelletti L. *Opt. Express*, **15**, 15250 (2007).
9. Zakharov P., Cardinaux F., Scheffold F. *Phys. Rev. E*, **73**, 011413 (2006).
10. Duri A., Sessoms D.A., Trappe V., Cipelletti L. *Phys. Rev. Lett.*, **102**, 085702 (2009).
11. Thompson C.A., Webb K.J., Weiner A.M. *J. Opt. Soc. Am. A*, **14**, 2269 (1997).
12. Zimnyakov D.A., Oh J.-T., Sinichkin Yu.P., Trifonov V.A., Gurianov E.V. *J. Opt. Soc. Am. A*, **21**, 59 (2004).
13. Zimnyakov D.A., Vilensky M.A. *Opt. Lett.*, **31**, 429 (2006).
14. Zimnyakov D.A., Sina J.S., Yuvchenko S.A., Isaeva E.A., Chekmasov S.P., Ushakova O.V. *Kvantovaya Elektron.*, **44**, 59 (2014) [*Quantum Electron.*, **44**, 59 (2014)].
15. Huang D., Swanson E.A., Lin C.P., Schuman J.S., Stinson W.G., Chang W., Hee M.R., Flotte T., Gregory K., Puliafito C.A., Fujimoto J.G. *Science*, **254**, 1178 (1991).
16. Wu J., Perelman L., Dasari R.R., Feld M.S. *Proc. Natl. Acad. Sci. USA*, **94**, 8783 (1997).
17. Zhang Q., Muller M.G., Wu J., Feld M.S. *Opt. Lett.*, **25**, 1451 (2000).
18. Bechger L., Koenderink A.F., Wos W.L. *Langmuir*, **18**, 2444 (2002).
19. Vogel R., Mereditth P., Harvey M.D., Rubinsztein-Dunlop H. *Spectrochimica Acta Part A*, **60**, 245 (2004).

20. Amelink A., Kruijt B., Robinson D.J., Sterenborg H.J.C.M. *J. Biomed. Opt.*, **13**, 054051 (2008).
21. Ishimaru A. *Wave Propagation and Scattering in Random Media* (San Diego, CA: Academic Press, 1978).
22. Goodman J.W. *Statistical Optics* (New York: Wiley Classics Library Edition, 2000).
23. http://omlc.org/spectra/PhotochemCAD/html/083.html (2012).
24. Henyey L.G., Greenstein J.L. *Astrophys. J.*, **93**, 70 (1941).
25. Van der Molen K.L., Mosk A.P., Lagendijk A. *Opt. Commun.*, **278**, 110 (2007).
26. Kim J.L., Liu Y., Roy H.K., Wali R.K., Backman V. *Opt. Lett.*, **29**, 1906 (2004).
27. Zimnyakov D.A., Pravdin A.B., Kuznetsova L.A., Kochubey V.I., Tuchin V.V., Wang R.K., Ushakova O.V. *J. Opt. Soc. Am. A*, **24**, 711 (2007).
28. Zimnyakov D.A., Yuvchenko S.A., Sina J.S., Ushakova O.V. *Pis'ma Zh. Eksp. Teor. Fiz.*, **98**, 366 (2013) [*JETP Lett.*, **98** (6), 326 (2013)].